Behavioral/Systems/Cognitive

5-HT_{1A} Receptor-Responsive Pedunculopontine Tegmental Neurons Suppress REM Sleep and Respiratory Motor Activity

Kevin P. Grace,[1] Hattie Liu,[2] and Richard L. Horner[1,2]
Departments of [1]Physiology and [2]Medicine, University of Toronto, Toronto, Ontario M5S 1A8, Canada

Serotonin type 1A (5-HT_{1A}) receptor-responsive neurons in the pedunculopontine tegmental nucleus (PPTn) become maximally active immediately before and during rapid eye movement (REM) sleep. A prevailing model of REM sleep generation indicates that activation of such neurons contributes significantly to the generation of REM sleep, and if correct then inactivation of such neurons ought to suppress REM sleep. We test this hypothesis using bilateral microperfusion of the 5-HT_{1A} receptor agonist 8-hydroxy-2-(di-*n*-propylamino)tetralin (8-OH-DPAT, 10 μM) into the PPTn; this tool has been shown to selectively silence REM sleep-active PPTn neurons while the activity of wake/REM sleep-active PPTn neurons is unaffected. Contrary to the prevailing model, bilateral microperfusion of 8-OH-DPAT into the PPTn ($n = 23$ rats) significantly increased REM sleep both as a percentage of the total recording time and sleep time, compared with both within-animal vehicle controls and between-animal time-controls. This increased REM sleep resulted from an increased frequency of REM sleep bouts but not their duration, indicating an effect on mechanisms of REM sleep initiation but not maintenance. Furthermore, an increased proportion of the REM sleep bouts stemmed from periods of low REM sleep drive quantified electrographically. Targeted suppression of 5-HT_{1A} receptor-responsive PPTn neurons also increased respiratory rate and respiratory-related genioglossus activity, and increased the frequency and amplitude of the sporadic genioglossus activations occurring during REM sleep. These data indicate that 5-HT_{1A} receptor-responsive PPTn neurons normally function to restrain REM sleep by elevating the drive threshold for REM sleep induction, and restrain the expression of respiratory rate and motor activities.

Introduction

Rapid eye movement (REM) sleep is a distinct brain state yet the mechanisms underlying its generation are unresolved. Neurons located in the pedunculopontine tegmental nucleus (PPTn) that discharge maximally immediately before, and during, REM sleep ("REM sleep-active") are thought significant to generating the state; the prevailing hypothesis being that REM sleep-active PPTn neurons generate REM sleep via cholinergic innervation and activation of pontine reticular formation (PRF) neurons, which themselves gate entry into REM sleep (Hobson et al., 2000; Lydic and Baghdoyan, 2003; Steriade and McCarley, 2005b). This hypothesis stems, primarily, from the evidence showing that pontine cholinergic mechanisms have the capacity to influence REM sleep expression. Evidence includes enhancement of REM sleep following cholinergic stimulation of the PRF, elevated PRF acetylcholine concentrations during REM sleep and following PPTn electrical stimulation, PPTn projections to the PRF, and the activity profile of REM sleep-active PPTn neurons being consistent with their involvement in REM sleep generation (Hobson et al., 2000; Lydic and Baghdoyan, 2003; Steriade and McCarley, 2005b).

These and other data, however, are not sufficient to establish that REM sleep-active PPTn neurons actually generate REM sleep for two reasons. First, these data do not preclude the alternative hypothesis that REM sleep-active PPTn neurons either have no effect on, or even suppress, REM sleep. Second, determination of the functional role of REM sleep-active PPTn in REM sleep generation requires identification of the effects of selective inhibition of this population of PPTn neurons, with the expectation that this intervention would suppress REM sleep according to the prevailing hypothesis. In each case, data contrary to the prevailing hypothesis of REM sleep generation would require significant revision of the current view.

Despite studies showing that pontine cholinergic mechanisms have the capacity to influence REM sleep expression, there is accumulating evidence that this is not the mechanism by which REM sleep-active PPTn neurons regulate REM sleep. For example, cholinergic stimulation of the PRF in rodents does not reliably enhance REM sleep, inducing wakefulness or having no effect in many cases (Bourgin et al., 1995; Deurveilher et al., 1997; Boissard et al., 2002; Pollock and Mistlberger, 2005), and endogenous acetylcholine in the PRF has not been shown necessary for REM sleep generation as tested by focal application of acetylcho-

Received Oct. 28, 2010; revised Nov. 23, 2011; accepted Dec. 5, 2011.

Author contributions: K.P.G. and R.L.H. designed research; K.P.G. and H.L. performed research; K.P.G. analyzed data; K.P.G. and R.L.H. wrote the paper.

This work was supported by funds from the Canadian Institutes of Health Research (Grant MT-15563). R.L.H. is supported by a Tier I Canada Research Chair in Sleep and Respiratory Neurobiology. K.G. is supported by a graduate studentship from the Ontario Thoracic Society. We thank Dr. Ralph Lydic, University of Michigan, Ann Arbor, for advice on the NADPH-diaphorase histochemistry.

Correspondence should be addressed to Dr. Richard L. Horner, Room 3206 Medical Sciences Building, 1 King's College Circle, Toronto, ON, Canada M5S 1A8. E-mail: richard.horner@utoronto.ca.

DOI:10.1523/JNEUROSCI.5700-10.2012

Copyright © 2012 the authors 0270-6474/12/321622-12$15.00/0

line receptor antagonists. REM sleep-active PPTn neurons are also predominately noncholinergic (Maloney et al., 1999; Verret et al., 2005). Spatially restricted PPTn lesions increase, rather than decrease, REM sleep (Lu et al., 2006), and $GABA_A$ receptor-mediated inhibition of PPTn neurons also increases REM sleep, with $GABA_A$ receptor antagonism having the opposite effect (Torterolo et al., 2002; Pal and Mallick, 2004, 2009). Overall, these data are inconsistent with the hypothesis that PPTn neurons promote REM sleep generation, but are limited by the nonselective nature of the interventions at the PPTn.

In light of the above findings contradicting the prevailing hypothesis regarding involvement of REM sleep-active PPTn neurons in REM sleep generation, we hypothesize that selective inhibition of REM sleep-active PPTn neurons (Thakkar et al., 1998) will show that this cell group functions to suppress REM sleep and its phenomenological components.

Materials and Methods

Animal care

Experiments were performed on a total of 29 male Wistar rats (Charles River) (mean body weight = 286.4 ± 2.01 g, range 270–304 g). Procedures conformed to the recommendations of the Canadian Council on Animal Care and the University of Toronto Animal Care Committee approved the protocols. Rats were housed individually, maintained on a 12 h light/dark cycle (lights on at 7:00 A.M.), and had *ad libitum* access to food and water.

Anesthesia and surgical procedures

Sterile surgery was performed under general anesthesia induced with isoflurane (3.5%). Rats were intraperitoneally injected with buprenorphine ($0.03\ mg \cdot kg^{-1}$) to minimize postoperative pain, atropine sulfate ($1\ mg \cdot kg^{-1}$) to minimize airway secretions, and saline (3 ml, 0.9%) for fluid loading. A surgical plane of anesthesia, as judged by abolition of the pedal withdrawal and corneal blink reflexes, was maintained with isoflurane (2–2.5%) administered with an anesthesia mask placed over the snout. The rats were then implanted with EEG and neck EMG electrodes for the determination of sleep–wake states, and with genioglossus and diaphragm electrodes for respiratory muscle recording (Steenland et al., 2008). Genioglossus muscle electrodes were considered correctly positioned if their electrical stimulation produced apical tongue contraction. It has been shown previously using sections of the medial branches of the hypoglossal nerves that genioglossus activity is recorded with such electrode placements (Morrison et al., 2002).

Using a stereotaxic apparatus (Kopf Model 962) microdialysis guides (CMA/11, Chromatography Sciences Company Inc.) were inserted into the brain bilaterally and positioned 4 mm above the caudal-most part of the PPTn pars compacta region (Rye et al., 1987; Paxinos and Watson, 1998). The following stereotaxic coordinates were used for guide placement: 0.57 mm anterior to lambda, 2 mm lateral to the midline, and 3.75 mm ventral to lambda. This site was chosen because a review of the literature showed that the region of the PPTn from its caudal border with the parabrachial complex to the nearest coronal section at which the decussation of the superior cerebellar peduncle is fully elaborated has the necessary connectivity to modulate REM sleep and its respiratory phenotype. This caudal pole of the PPTn is neurophysiologically distinct, since unlike more rostral PPTn locations, neurons in this caudal region are REM sleep-active, project to the PRF (Jones, 1990; Semba et al., 1990; Semba and Fibiger, 1992; Kohlmeier et al., 2002) and thalamus (Semba et al., 1990; Semba and Fibiger, 1992; Bevan and Bolam, 1995), and are thought to modulate REM sleep and the associated electrocortical activation (Steriade and McCarley, 2005a,b). Neurons in the caudal pole of the PPTn also project to the areas of the rostral ventrolateral medulla (Yasui et al., 1990) that contain respiratory neurons critical to the generation of respiratory rhythm and pattern (Feldman and Del Negro, 2006), and to motor pools such as the hypoglossal motor nucleus which innervates the genioglossus muscle of the tongue (Woolf and Butcher, 1989; Fay and Norgren, 1997; Rukhadze and Kubin, 2007).

At the end of surgery, all the electrodes were connected to pins and inserted into a miniature plug (STC-89PI-220ABS, Carleton University, Ottawa, ON, Canada). The plug and microdialysis guides were then affixed to the skull with dental acrylic and anchor screws. The rats were given 7–8 d to recover before any experiments were performed.

Habituation and recording procedures

The evening before the experiment (7:00 P.M., i.e., the beginning of the dark/active period), the rats were placed in the recording environment for the purpose of habituation. The recording environment consisted of an large open-topped bowl (Rodent Bowl, MD-1514, BAS Inc.) mounted on a modified stand-alone turntable (Rat Turn, MD-1404, BAS Inc.), housed within a noise-attenuated, electrically shielded cubicle (EPC-010, BRS/LVE Inc.). A light-weight counterbalanced recording cable was connected to the headpiece of the rat. Twisting of the microdialysis tubing and recording cable resulting from rotational movement of the animal was prevented by compensatory rotation of the turntable apparatus as necessary. Rats were provided food and water *ad libitum* throughout the study. A video camera located within the cubicle allowed for continuous visual monitoring without disturbing the animal.

Microdialysis

On the morning of the experiments, at ~10:00 A.M., the internal cannulae were removed from the guides and microdialysis probes (CMA/11 14/01) were inserted. The probes projected 4 mm from the tip of the guide and were so targeted to the caudal-most part of the PPTn pars compacta region bilaterally (described in the section Anesthesia and surgical procedures). The probes were 240 μm in diameter with a 1 mm cuprophane membrane and a 6000 Da cutoff. Each probe was connected to FEP Teflon tubing (inside diameter, 0.12 mm) with this tubing connected to 1.0 ml syringes via a zero dead space switch (Uniswitch, BAS Inc.). The probes were continuously flushed with artificial CSF (ACSF) at a flow rate of $2.1\ \mu l \cdot min^{-1}$ using a syringe pump and controller (MD-1001 and MD1020, BAS Inc.). The composition of ACSF was (in mM): 125 NaCl, 3 KCl, 1 KH_2PO_4, 2 $CaCl_2$, 1 $MgSO_4$, 25 $NaHCO_3$, and 30 D-glucose. The ACSF was warmed to 37°C and bubbled with CO_2 to a pH of 7.38 ± 0.005. The $CaCl_2$ was added after adjusting the temperature and pH.

Protocol

All experiments were performed during the day when rats normally sleep. To help ensure that sleep architecture had normalized after probe insertion before the recording of baseline values, data obtained in the first 2 h following probe insertion were excluded from the analyses in all rats. In three of 29 rats disruption of sleep was still evident in the second hour following probe insertion as judged by wakefulness accounting for >63% of the total recording time during perfusion of ACSF, i.e., 3 SDs greater than the mean proportion of wakefulness. Accordingly, these three rats were excluded from the analysis of sleep architecture per se, which was an a priori decision made regardless of the sleep/wake architecture responses to subsequent manipulation of the PPTn. Nevertheless, the data from these three rats were still included in the analysis of state phenomenology (i.e., the postural and respiratory muscle activities, respiratory rate, and electrocortical activity that occurred within each sleep–wake state) because these state-specific phenomena depend on the presence of the state rather than the amount of its occurrence.

The entire experimental protocol occurred over a 5 h period (12:00–5:00 P.M.). Two hours of data were collected for each experimental condition (i.e., ACSF and drug intervention). Data obtained in the hour following switching of the microdialysis perfusate were excluded from all analyses. Since transitioning between behavioral states is sometimes associated with ambiguity in sleep–wake state determination and unstable breathing, the following exclusion criteria were adopted to help ensure that all data included in the analysis of state phenomenology were obtained from temporally enduring periods within unequivocally defined sleep–wake states: (1) all bouts of REM sleep and wakefulness lasting <30 s, and all bouts of non-REM sleep lasting <60 s were excluded from the analysis of state phenomenology, (2) if a state transition occurred during a scoring epoch then that epoch was also excluded from the analysis of state phenomenology.

Following baseline recordings, during which time the PPTn was perfused with ACSF, the perfusion medium was either maintained as ACSF without drug (i.e., time control, $n = 11$ rats) or switched to perfusion of: (1) the type 1A serotonin (5-HT_{1A}) receptor agonist (±) 8-hydroxy-2-(di-*n*-propylamino) tetralin (8-OH-DPAT, 10 μM in ACSF, Sigma) in a group of 12 rats, or (2) the selective 5-HT_{1A} receptor antagonist (*S*)-WAY 100135 (1 μM in ACSF, Tocris Bioscience) in 6 rats. The time control group was included to determine whether any changes in sleep occurring during 8-OH-DPAT perfusion stemmed from time-of-day influences on sleep–wake state architecture independent of an 8-OH-DPAT effect per se. A concentration of 10 μM 8-OH-DPAT was chosen for this study because a previous study in cats using the same technique of reverse microdialysis at the PPTn combined with simultaneous unit recording of PPTn neurons showed that this concentration of 8-OH-DPAT selectively silenced the activity of REM sleep-active PPTn neurons while the discharge of wake/REM sleep-active PPTn neurons was unaffected (Thakkar et al., 1998). 5-HT_{1A} receptor expression is thought to be the principal characteristic distinguishing PPTn wake/REM sleep-active neurons from REM sleep-active neurons (Thakkar et al., 1998; Steriade and McCarley, 2005b). WAY 100135 was microperfused at a concentration of 1 μM because this concentration should produce tissue concentrations above (*S*)-WAY 100135's binding affinity for the 5-HT_{1A} receptor ($IC_{50} = 15$ nM) but well below the binding affinities for other monoaminergic receptor subtypes ($IC_{50} > 1000$ nM) (Fletcher et al., 1993).

At the end of each experiment, rats were killed with an overdose of isoflurane (5% administered for ~20 min) and perfused intracardially with 0.1 M PBS and 4% paraformaldehyde. The microdialysis guides and probes remained in place during the fixing procedure because it made for straightforward anatomical identification of the site of microdialysis. Location of the site of microdialysis allowed us to identify the relationships between probe location and the magnitude of the effect on REM sleep produced by 8-OH-DPAT at the PPTn (see Results). After fixing, the brains were removed and fixed overnight in a 1:1 solution of 4% paraformaldehyde and PBS. Brains were then transferred to a 30% sucrose solution for 24 h, after which they were rapidly frozen and cut into 50 μM coronal sections with a cryostat (Leica CM 1850).

The PPTn is neuroanatomically defined by its cholinergic cell population (Rye et al., 1987), and so to verify that microdialysis probes were correctly located, PPTn cholinergic cells were identified using NADPH-diaphorase histochemistry. Although described in more detail previously (Vincent et al., 1983), slide-mounted sections were incubated in a solution composed of 0.1% NADPH (Sigma N-6505), 0.01% nitro blue tetrazolium (Sigma N-6876), and 0.3% Triton X-100 (Sigma) in 0.05 M Tris-buffered saline, pH 7.4, for 30 min at 37°C. Sections were then counterstained with neutral red and microdialysis probe sites were determined from the stained sections. Microdialysis probe sites were marked on standard brain maps (Paxinos and Watson, 1998).

As an additional test of whether the effects of 8-OH-DPAT on REM sleep involved the PPTn, the distances between the center of the sites of microdialysis and the PPTn pars compacta (distances calculated by trigonometry) were correlated for each animal with the magnitude of changes in REM sleep time as a percentage of total sleep time during 8-OH-DPAT perfusion. The center of the site of microdialysis was taken as the point on the histological section 0.5 mm above the ventral tip of the microdialysis perfusion site (probe length being 1 mm). The position of the PPTn pars compacta was taken as the center point of the PPTn cholinergic cell mass (as determined by NADPH-diaphorase histochemistry) on the brain section having the most numerous population of cholinergic cells adjacent to the superior cerebellar peduncle (i.e., the PPTn). Brain sections were visualized and the sites of microdialysis analyzed using Infinity Capture and Analyze software packages (Lumenara). Based on the hypothesis of this study, a significant negative correlation would be expected if the PPTn was associated with the responses; the absence of a significant correlation would indicate that changes in REM sleep during 8-OH-DPAT perfusion are the product of 8-OH-DPAT acting at a site other than the PPTn.

Recording procedures

The electrical signals were amplified and filtered (Super-Z head-stage amplifiers and BMA-400 amplifiers/filters, CWE Inc.). The EEG was filtered between 1 and 100 Hz, whereas neck, genioglossus and diaphragm EMGs were filtered between 100 and 1000 Hz. The electrocardiogram was removed from the diaphragm EMG using an oscilloscope and electronic blanker (Model SB-1, CWE Inc.). The moving-time averages (time constant = 200 ms) of the EMGs were also obtained (Model MA-821, CWE Inc.). Each signal was digitized and recorded on computer (Spike 2 software, 1401 interface, CED Ltd).

Data analysis

EMG and EEG signals. The data were analyzed in consecutive 5 s time-bins. The genioglossus, diaphragm and neck EMG signals were analyzed from the respective moving-time average signals (above electrical zero) and were quantified in arbitrary units. Electrical zero was the voltage recorded with the amplifier inputs grounded. The genioglossus and diaphragm signals were analyzed on a breath-by-breath basis which corresponded to ~7–10 breaths for each 5 s epoch. For each breath, the analysis of the genioglossus EMG was time-locked to breathing as defined by the peak and trough of the diaphragm signal. Genioglossus activity was quantified as mean tonic activity (i.e., basal activity in expiration) and respiratory-related activity (i.e., peak inspiratory activity − tonic activity), and average values for these measures of genioglossus activity were calculated. Mean neck muscle activity, diaphragm amplitude and respiratory rate were also calculated in the same consecutive 5 s time-bins for all the periods of sleep and wakefulness in each rat. One rat was excluded from the analysis of genioglossus muscle activity as no respiratory-related activity was recorded under any circumstances during the experiment, which is highly atypical of the rats in this and other studies from our laboratory (Sood et al., 2005; Chan et al., 2006; Younes et al., 2007; Steenland et al., 2008), and as such was a possible indicator that the electrodes were in a different tongue muscle in that animal. In addition, in the potential event of there being little effect of 8-OH-DPAT on the amplitude of respiratory-related genioglossus, such a minimal effect could not be reliably attributed to a lack of drug effect per se and may simply have been due to the fact that there was little/no signal to suppress.

Additional analyses of genioglossus activity were performed in REM sleep because the rhythmic respiratory modulation of the genioglossus which typically persists throughout wakefulness and non-REM sleep is often absent during normal REM sleep and sporadic muscle twitching, not obviously related to diaphragm activation, predominates. Accordingly, these REM sleep-specific muscle twitching events in the genioglossus as well as the non-respiratory muscle of the neck were analyzed by an additional procedure. Muscle twitching activity was analyzed from the rectified raw genioglossus and neck muscle signals followed by derivation of the moving time average signal using a shorter time constant of 30 ms. The background tonic activity was removed by filtering, thereby isolating muscle twitches from the other components of the signal. Upon isolating the muscle twitches, the amplitude of these phasic motor events was calculated.

The EEG was sampled at 2000 Hz then analyzed on overlapping segments of 1024 samples, windowed using a raised cosine (Hamming) function and subjected to fast Fourier transform to yield the power spectrum. The window was advanced in steps of 512 samples, and the mean power spectrum of the EEG signal over each 5 s epoch was calculated. The power contained within six frequency bands was recorded as absolute power and also as a percentage of the total power of the signal. The band limits were δ_2 (0.5–2 Hz), δ_1 (2–4 Hz), θ (4–7.5 Hz), α (7.5–13.5 Hz), β_1 (13.5–20 Hz), β_2 (20–30 Hz).

Identification of sleep–wake states. Sleep–wake states were identified by visual inspection and classified into wakefulness, non-REM, and REM sleep according to standard scoring criteria (Horner et al., 1997; Horner et al., 1998). All periods of wakefulness in which rats were eating, drinking, grooming or engaged in some overt behavior were classified as active wakefulness. Periods of wakefulness being characterized by relatively little or no behavioral activity were classified as quiet wakefulness. During active wakefulness, the diaphragm EMG recordings can become contam-

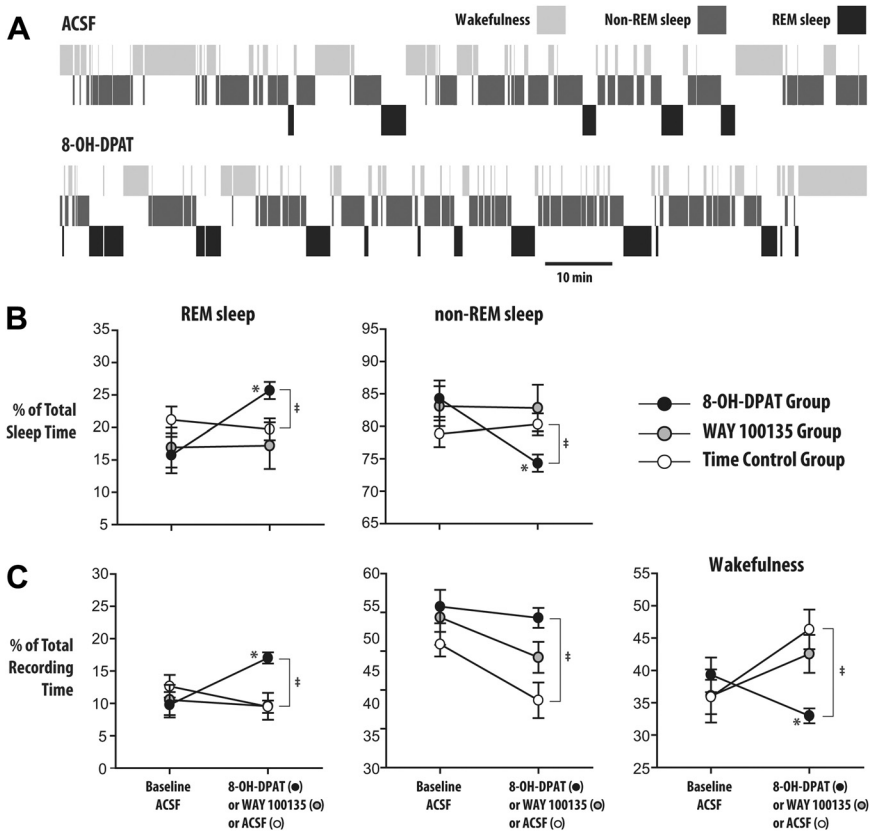

Figure 1. Inhibition of 5-HT_{1A} receptor-responsive PPTn neurons increases REM sleep. ***A***, Example hypnograms from a single rat showing the distribution of sleep–wake states over a 2 h period with microperfusion of ACSF and 8-OH-DPAT into the PPTn. ***B***, Group data showing the amounts of REM sleep and non-REM sleep as a percentage of the total sleep time in the presence of ACSF, 8-OH-DPAT, and WAY 100135 at the PPTn. ***C***, Group data showing the amounts of REM sleep, non-REM sleep and wakefulness as a percentage of the total recording time in the presence of ACSF, 8-OH-DPAT, and WAY 100135 at the PPTn. Values are means ± SEM. *$p < 0.05$ from within-animal baseline ACSF control; ‡$p < 0.05$ from between-animal ACSF time controls.

inated by movement-related artifacts and so periods of active wakefulness were excluded from analysis of respiratory variables since an inability to identify the peak and trough of each diaphragm breath prevents a meaningful analysis of diaphragm amplitude, respiratory rate, and respiratory-related genioglossus activity.

Analysis of sleep architecture. To indentify the role of REM sleep-active PPTn neurons in shaping sleep architecture we quantified wakefulness, non-REM and REM sleep as percentages of the total recording time (2 h; see above for data collection and inclusion criteria). Amounts of non-REM and REM sleep were also calculated as a percentage of total sleep time (i.e., independent of wakefulness). The mean bout frequency and duration for each sleep–wake state was also calculated.

We aimed to identify whether or not REM sleep-active PPTn neurons exert control over two important factors in REM sleep initiation, namely, the strength of REM sleep drive which builds before, and is responsible for, REM sleep onset, as well as the threshold level of the drive which need be breached to trigger REM sleep onset. We used an algorithm developed by Benington and Heller (Benington and Heller, 1994; Benington et al., 1994) to quantify the strength of REM sleep drive during non-REM to REM sleep transitions (NRTs) by determining the magnitude of stereotypical electrographic changes that herald the onset of REM sleep. More specifically, the algorithm identifies periods of non-REM sleep lasting at least 40 s, in which EEG delta power is declining while theta and alpha power is high. From these electrographic variables, a score termed the non-REM to REM sleep transition indicator value (NIV) is calculated for each NRT. The NIV is a valid indicator of relative REM sleep drive since a high NIV is associated with a high likelihood of successful transitioning from non-REM to REM sleep, and values increases as a function of time since the last REM sleep episode (Benington and Heller, 1994; Benington et al., 1994).

We defined a NIV threshold to demarcate between periods of high and low REM sleep drive as follows. Each NIV score was converted to a percentage of the maximum NIV score obtained under control conditions in the same animal. NIV scores from all animals were then pooled into bins of equal width (i.e., 0–20% of maximum NIV, 20–40% of maximum NIV, etc.). The percentage of successful REM sleep onsets was calculated for each bin as the number of NRTs immediately proceeded by a bout of REM sleep divided by the total number of NRTs (Benington and Heller, 1994; Benington et al., 1994). The histogram of successful REM sleep onset percentage versus normalized NIV describes a sigmoid curve, with high normalized NIVs being associated with a high likelihood of REM sleep onset (Benington and Heller, 1994; Benington et al., 1994). The demarcation threshold is equivalent to the normalized NIV level at which the slope of the NIV versus successful REM sleep onset curve is maximal (Benington and Heller, 1994; Benington et al., 1994). By applying this threshold to the pool of REM sleep bouts from each animal the percentage of REM sleep bouts issuing from periods of low versus high REM sleep drive was calculated. Any changes in the relative level of REM sleep drive required to successfully initiate REM sleep can be taken as an indication of changes in REM sleep induction threshold. In some cases bouts of REM sleep can be immediately followed by another REM sleep bout usually of very short duration. This phenomenon is known as REM sleep clustering (Amici et al., 2000). We defined REM sleep clusters as two or more REM sleep bouts being separated by <60 s. For the purposes of this analysis, we considered a REM sleep cluster as single, although fragmented, episode of REM sleep.

Averaging data within and between rats. Each rat served as its own control with all interventions performed in one experiment, therefore allowing for consistent effects of experimental condition (e.g., ACSF followed by 8-OH-DPAT or ACSF) to be observed across sleep–wake states within and between rats. Data collected during wakefulness, non-REM and REM sleep were analyzed for each experimental condition in each rat. Then for each animal a grand mean was calculated for each variable, for each sleep–wake state, and for each drug delivered to the PPTn.

Statistical analysis. The analyses performed for each statistical test are included in the text where appropriate. For the two-way ANOVAs with repeated measures (ANOVA-RM), the two factors to determine effects on sleep architecture were Treatment (i.e., ACSF vs 8-OH-DPAT or WAY 100135) and Time, i.e., baseline (ACSF control) and intervention (8-OH-DPAT, or WAY 100135, or ACSF time control). For analyses of respiratory rate and motor activities across states of wakefulness, non-REM and REM sleep, the two factors were Treatment and State. Where *post hoc* comparisons were performed after ANOVA-RM, the Bonferroni-corrected *p*-value was used to test statistical significance. Differences were considered significant if the null hypothesis was rejected at $p < 0.05$. Analyses were performed using SigmaStat (SPSS).

Results

Effects on REM sleep amounts

Figure 1 shows that bilateral microperfusion of 8-OH-DPAT into the PPTn of these freely behaving rats caused a robust increase in REM sleep, whether expressed as a percentage of the total sleep time or total recording time.

The amount of REM sleep as a percentage of the total sleep time was significantly changed by the interventions at the PPTn (interaction effect between Treatment and Time: $F_{(1,17)} = 8.21$, $p = 0.011$, two-way ANOVA-RM). *Post hoc* analyses showed that the percentage of the total sleep time occupied by REM sleep in the presence of 8-OH-DPAT at the PPTn was significantly increased compared with both the within-animal baseline ACSF control ($p = 0.003$, *post hoc* paired *t* test, Fig. 1*B*) and the between-animal ACSF time controls ($p = 0.045$, *post hoc* unpaired *t* test, Fig. 1*B*). As expected there was no difference between the amounts of REM sleep recorded in the presence of ACSF at the PPTn in both the within-animal baseline ACSF control ($p = 0.600$, *post hoc* paired *t* test, Fig. 1*B*) and the between-animal ACSF time controls ($p = 0.067$, *post hoc* unpaired *t* test, Fig. 1*B*). WAY 100135 at the PPTn did not affect REM sleep as a percentage of total sleep time (Fig. 1*B*, main effect of Treatment: $F_{(1,14)} = 1.44$, $p = 0.250$; main effect of Time: $F_{(1,14)} = 0.08$, $p = 0.783$; interaction effect between Treatment and Time: $F_{(1,14)} = 0.17$, $p = 0.684$, two-way ANOVA-RM). Given that in the available sleep period the time not occupied by REM sleep will (by definition) be occupied by non-REM sleep, the same significant differences also apply to effects on non-REM sleep, i.e., with the significant increases in REM sleep with 8-OH-DPAT at the PPTn there were corresponding decreases in non-REM sleep (Fig. 1*B*).

The increases in REM sleep with 8-OH-DPAT at the PPTn persisted when the analyses were extended to include the effects on sleep–wake states as a percentage of the total recording time (interaction effect between Treatment and Time: $F_{(1,17)} = 12.29$, $p = 0.003$, two-way ANOVA-RM, Fig. 1*C*). The percentage recording time occupied by REM sleep with 8-OH-DPAT at the PPTn was higher compared with the within-animal baseline ACSF control ($p = 0.004$, *post hoc* paired *t* test, Fig. 1*C*) and the between-animal ACSF time controls ($p < 0.001$, *post hoc* unpaired *t* test, Fig. 1*C*). As expected, there was no difference between the amounts of REM sleep recorded with ACSF at the PPTn in the within-animal baseline ACSF controls ($p = 0.140$, *post hoc* paired *t* test, Fig. 1*C*) and the between-animal ACSF time controls ($p = 0.174$, *post hoc* unpaired *t* test, Fig. 1*C*). Amounts of REM sleep as a percentage of total recording time in the WAY 100135 group were statistically indistinguishable from the ACSF control group (Fig. 1*B*, main effect of Treatment: $F_{(1,14)} = 0.29$, $p = 0.602$; main effect of Time: $F_{(1,14)} = 1.71$, $p = 0.212$; interaction effect between Treatment and Time: $F_{(1,14)} = 0.48$, $p = 0.499$, two-way ANOVA-RM).

With the significant increase in REM sleep with 8-OH-DPAT at the PPTn, the amounts of wakefulness and non-REM sleep as a percentage of the total recording time were also necessarily affected. Figure 1*C* includes the effects on wakefulness (interaction effect between Treatment and Time: $F_{(1,17)} = 19.59$, $p < 0.001$, two-way ANOVA-RM; $p = 0.034$, *post hoc* paired *t* test between 8-OH-DPAT and the within-animal baseline ACSF control; $p < 0.001$, *post hoc* unpaired *t* test between 8-OH-DPAT and the between-animal ACSF time control). As expected, there was no difference in the amount of wakefulness recorded pretreatment, i.e., under baseline conditions in the presence of ACSF at the PPTn in both groups of animals ($p = 0.349$, *post hoc* unpaired *t* test, Fig. 1*C*). There was, however, an increase in the amount of wakefulness recorded in the presence of continued ACSF at the PPTn, i.e., the within-animal ACSF time control group ($p < 0.001$, *post hoc* paired *t* test, Fig. 1*C*). This result indicates that wakefulness normally increases in the recording period in the absence of the 8-OH-DPAT intervention at the PPTn, such that the decrease in the presence of 8-OH-DPAT is related to accommodating the significant increases in REM sleep (Fig. 1*B*,*C*). This decreased wakefulness in the presence of 8-OH-DPAT is likely not explained by inadvertent inactivation of wakefulness-promoting wake/REM sleep-active PPTn cell population because of the evidence in cat that this PPTn subpopulation is unaffected by 8-OH-DPAT (Thakkar et al., 1998). This analysis suggests, therefore, that the decreased wakefulness is the consequence of the increased amounts of REM sleep and not the cause of the increased REM sleep, an analysis supported by the result that increased REM sleep also occurred when quantified as a percentage of the total sleep time (i.e., regardless of wakefulness, Fig. 1*B*).

Figure 1*C* also includes the effects on non-REM sleep as a percentage of the total recording time (interaction effect between Treatment and Time: $F_{(1,17)} = 5.23$, $p = 0.035$, two-way ANOVA-RM). There was no change in non-REM sleep with 8-OH-DPAT as a percentage of the recording time ($p = 0.439$, *post hoc* paired *t* test between 8-OH-DPAT and the within-animal baseline ACSF control), showing that the increased sleep was attributed mainly to the aforementioned increased REM sleep (Fig. 1*B*,*C*). There was also no difference in the amount of non-REM sleep recorded pretreatment, i.e., under baseline conditions in the presence of ACSF at the PPTn in both groups of animals ($p = 0.081$, *post hoc* unpaired *t* test, Fig. 1*C*).

In the WAY 100135 group, changes in wakefulness and non-REM sleep were statistically indistinguishable from the time control group (Fig. 1*B*, for wake and non-REM sleep, respectively, main effects of Treatment: $F_{(1,14)} = 0.24$, $p = 0.636$ and $F_{(1,14)} = 2.41$, $p = 0.143$; main effects of Time: $F_{(1,14)} = 10.01$, $p = 0.007$ and $F_{(1,14)} = 12.69$, $p = 0.003$; interaction effects between Treatment and Time: $F_{(1,14)} = 0.54$, $p = 0.475$, and $F_{(1,14)} = 0.36$, $p = 0.559$, two-way ANOVA-RM).

Intervention sites and relationship to the magnitude of effect on REM sleep

Figure 2*A–C* shows an example and group data indicating the locations of the microdialysis probe sites from all experiments with 8-OH-DPAT, WAY 100135 as well as the ACSF time controls. Figure 2*D* also shows that the relationship between the magnitude of the increase in REM sleep produced by microperfusion of 8-OH-DPAT was significantly correlated with the distance of the center of the intervention site from the PPTn ($r^2 = 0.659$ and 0.465 for the left and right-sided intervention sites, respectively, $p = 0.008$ and 0.043, Spearman rank order correlations).

Effects on REM sleep initiation versus maintenance

Figure 3 shows the effects of 8-OH-DPAT and WAY 100135 at the PPTn on the frequencies and durations of REM sleep bouts, relative to both the within-animal ACSF controls and the between-animal ACSF time-controls. These data illustrate that the increased REM sleep following bilateral microperfusion of 8-OH-DPAT into the PPTn was the result of an increased frequency of REM sleep bouts but not their duration.

REM sleep bout frequency was significantly affected by the interventions (interaction effect between Treatment and Time: $F_{(1,17)} = 23.68$, $p < 0.001$, two-way ANOVA-RM), being increased in the presence of 8-OH-DPAT at the PPTn compared with both the within-animal baseline ACSF controls ($p < 0.001$, *post hoc* paired *t* test, Fig. 3*A*) and the between-animal ACSF time controls ($p < 0.001$, *post hoc* unpaired *t* test, Fig. 3*A*). In contrast there was no effect of interventions at the PPTn on REM sleep bout length (Fig. 3*B*, main effect of Treatment: $F_{(1,17)} = 0.01$, $p = 0.916$; main effect of Time: $F_{(1,17)} = 0.001$, $p = 0.971$; inter-

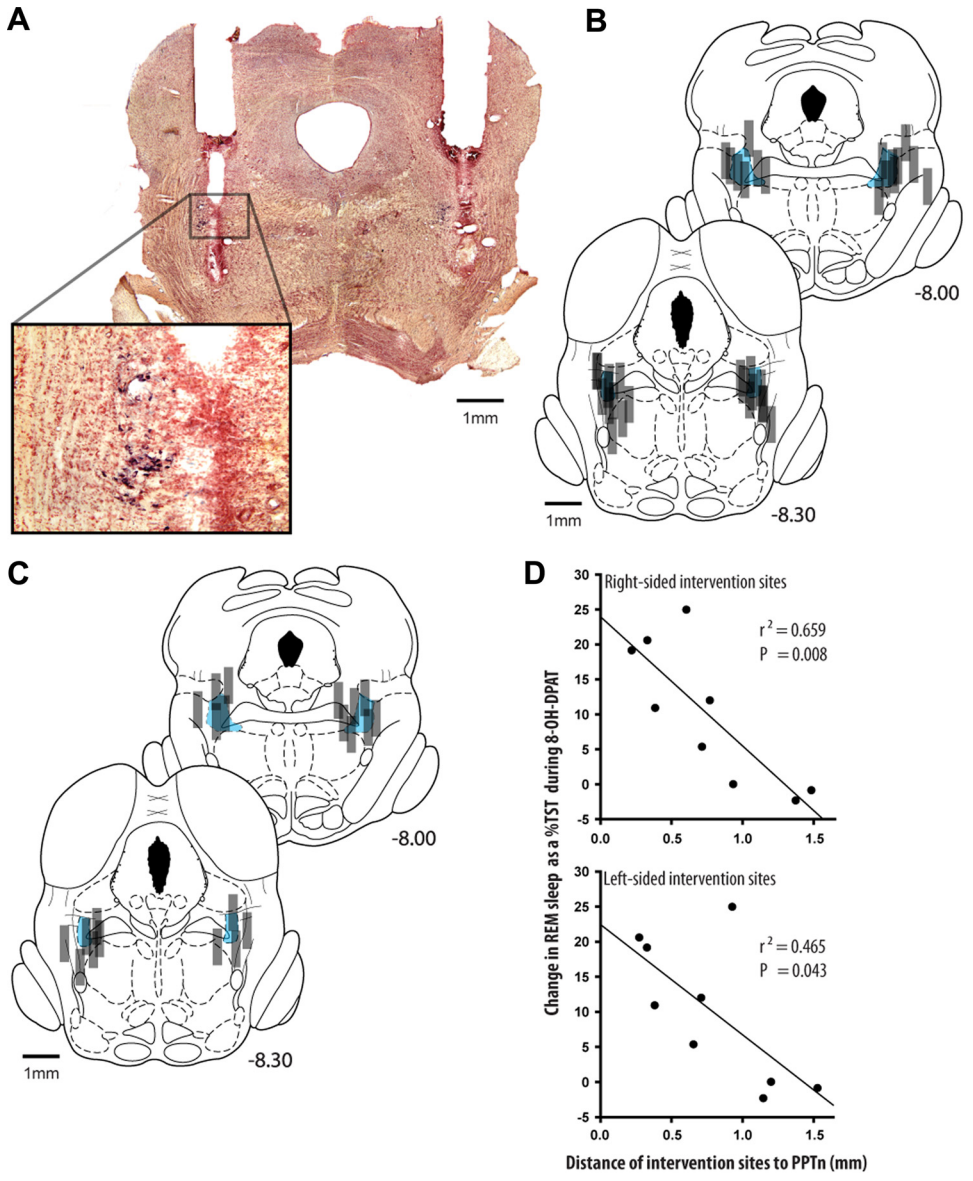

Figure 2. Location of interventions and relationship to REM sleep suppression. ***A–C***, Example (***A***) and group data showing the location of microdialysis probes from all experiments with bilateral microperfusion of 8-OH-DPAT and WAY 100135 into the PPTn (***B***) and the ACSF time-controls (***C***). The coronal tissue section in ***A*** also shows that the probe sites were located adjacent to NADPH-diaphorase-labeled cells of the PPTn. The gray rectangles in ***B*** and ***C*** represent the locations of the semipermeable membrane-tip of the microdialysis probes. ***D***, The significant relationships between the magnitude of the increase in REM sleep as a percentage of the total sleep time (TST) produced by microperfusion of 8-OH-DPAT and the distance from the center of the microdialysis membrane to the PPTn (shaded blue) (see Materials and Methods for further details).

action effect between Treatment and Time: $F_{(1,17)} = 0.07$, $p = 0.791$, two-way ANOVA-RM). As with REM sleep amounts, WAY 100135 had no effects on either REM sleep bout frequency or duration relative to the ACSF controls (Fig. 3*A*,*B*, for bout frequency and length, respectively, main effects of Treatment: $F_{(1,14)} = 0.245$, $p = 0.628$ and $F_{(1,14)} = 0.0172$, $p = 0.898$; main effects of Time: $F_{(1,14)} = 2.157$, $p = 0.164$ and $F_{(1,14)} = 0.396$, $p = 0.539$; interaction effects between Treatment and Time: $F_{(1,14)} = 0.379$, $p = 0.548$, and $F_{(1,14)} = 0.130$, $p = 0.723$, two-way ANOVA-RM).

In addition to 8-OH-DPAT at the PPTn producing more frequent bouts of REM sleep of unchanged duration (Fig. 3*A*,*B*), there were also associated changes in non-REM sleep and wakefulness episodes. Figure 3 includes the significant differences from the *post hoc* analyses which followed the two-way ANOVA-RMs for non-REM sleep bout frequency (interaction effect between Treatment and Time: $F_{(1,17)} = 4.52$, $p = 0.049$), wakefulness bout frequency (interaction effect between Treatment and Time: $F_{(1,17)} = 5.28$, $p = 0.035$), non-REM sleep durations (main effect of Time: $F_{(1,17)} = 24.87$, $p < 0.001$) and wakefulness durations (interaction effect between Treatment and Time: $F_{(1,17)} = 15.64$, $p = 0.001$). Figure 3 also shows the absence of effects of WAY 100135 on the frequency and duration of non-REM and wakefulness bouts relative to ACSF time controls (interaction effects between Treatment and Time: range of $F_{(1,14)} = 0.0284–0.464$, range of $p = 0.869–0.507$, two-way ANOVA-RM).

Effects on REM sleep drive threshold

The data above indicate that the increased REM sleep following bilateral microperfusion of 8-OH-DPAT into the PPTn was the result of an increased frequency of REM sleep bouts but not their duration, implicating an effect on mechanisms of REM sleep ini-

tiation but not maintenance (Benington and Heller, 1994; Benington et al., 1994). To further define the functional role of REM sleep-active PPTn neurons in REM sleep initiation we determined whether the observed increase in REM sleep during microperfusion of 8-OH-DPAT into the PPTn resulted from an increased REM sleep drive, as indexed by the NIVs calculated from the electroencephalographic frequencies during NRTs.

Figure 4 shows an example and group data for the variation of NIVs in the non-REM sleep periods preceding REM sleep for both ACSF and 8-OH-DPAT at the PPTn. Figure 4*B* shows the expected (Benington and Heller, 1994; Benington et al., 1994) sigmoid relationship between the calculated NIVs and the percentage of NRTs culminating in REM sleep bouts ($r^2 = 0.991$, $p = 0.013$, sigmoid curve fit). This relationship shows that high NIVs were associated with high probabilities of REM sleep onsets. The NIV threshold which demarcated periods of high and low REM sleep drive was taken as 40% (see Materials and Methods for determination of threshold). This NIV threshold has face validity as a predictor of a transition to REM sleep since under control conditions with ACSF at the PPTn, an average of 91.3 ± 3.5% of REM sleep episodes were preceded by NRTs with NIVs above this threshold.

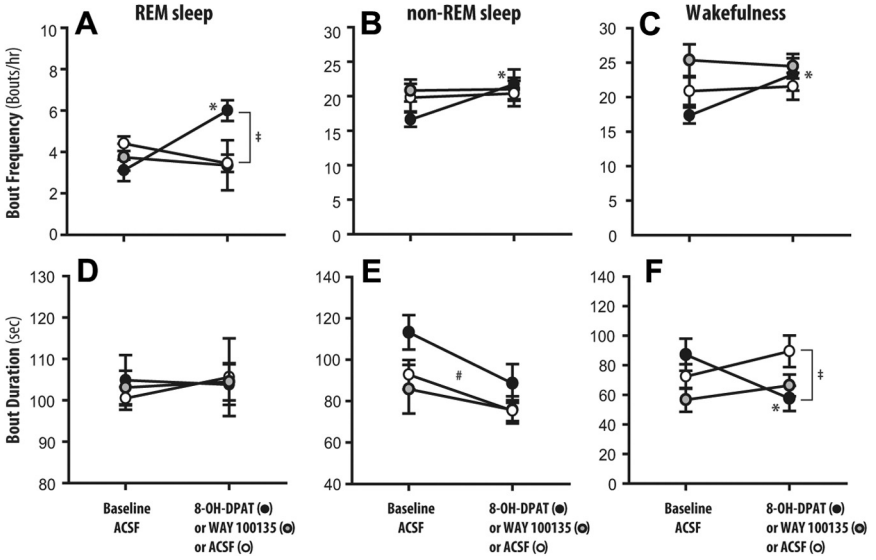

Figure 3. Group data showing the frequency and duration of REM sleep (***A***, ***D***), non-REM sleep (***B***, ***E***), and wakefulness (***C***, ***F***) bouts in the presence of ACSF, 8-OH-DPAT, and WAY 100135 at the PPTn. Values are means ± SEM. *$p < 0.05$ from within-animal baseline ACSF control; ‡$p < 0.05$ from between-animal ACSF time controls; #$p < 0.05$ main effect of Time, i.e., baseline ACSF control to intervention period (8-OH-DPAT or WAY 100135 or ACSF time control).

The representative hypnogram in Figure 4*A* (color coded for NIV values in non-REM sleep) illustrates that bouts of REM sleep in the presence of 8-OH-DPAT at the PPTn were more often preceded by periods of non-REM sleep with lower NIVs, indicative that a low REM sleep drive is now sufficient to transition to REM sleep. Importantly, the group data showed that the proportion of REM sleep episodes resulting from periods of low REM sleep drive was significantly increased from 8.7 ± 3.5% to 37.2 ± 9.7 in the presence of microperfusion of 8-OH-DPAT into the PPTn (Fig. 4*C*,$p = 0.019$, paired *t* test). Reciprocally, the proportion of REM sleep episodes resulting from periods of high REM sleep drive significantly decreased from 91.3 ± 3.5% to 62.8 ± 9.7% in the presence of microperfusion of 8-OH-DPAT into the PPTn (Fig. 4*C*,$p = 0.019$, paired *t* test). The proportion of REM sleep episodes resulting from periods of high REM sleep drive during WAY 100135 microperfusion (92.5 ± 4.8%) was not statistically different compared with ACSF controls (95.1 ± 3.1%, $p = 0.629$, paired *t* test), consistent with the lack of effects on other REM sleep measures during microperfusion of WAY 100135 into the PPTn. These data show that REM sleep was initiated more easily with 8-OH-DPAT at the PPTn, thereby indicating that under normal conditions (i.e., without 8-OH-DPAT), 5-HT_{1A} receptor-responsive PPTn neurons act to suppress REM sleep by increasing the threshold for its initiation, thereby preventing premature transitioning into REM sleep.

Finally, given that changes in EEG power per se (particularly in the α, δ, and θ frequency bands) could theoretically produce artifactual changes in calculated NIVs, we compared EEG power in the six frequency bands spanning 0.5–30 Hz between the 8-OH-DPAT and ACSF treatment conditions. There was no effect of 8-OH-DPAT (Fig. 5) or WAY 100135 at the PPTn on EEG power in any frequency band across the states of wakefulness, non-REM and REM sleep (for 8-OH-DPAT and WAY 100365 groups, main effect of Treatment: range of $F_{(1,11)} = 0.002–4.14$, range of $p = 0.963–0.067$, two-way ANOVA-RMs). These results show that the EEG was unchanged by 8-OH-DPAT at the PPTn, and the transitions from non-REM to REM sleep were simply initiated at lower NIVs in the presence of 8-OH-DPAT. Nevertheless, there were expected changes in EEG activity as a function of sleep–wake state, such as the decreased slow frequencies, and increased faster frequencies, in wakefulness and REM sleep compared with non-REM sleep. Figure 5 shows the significant changes in EEG frequencies across sleep–wake states as revealed by *post hoc* analyses following the two-way ANOVA-RMs. EEG frequencies and their changes with state in the WAY 100135 group were comparable to those shown in Figure 5 for the 8-OH-DPAT group.

Effects on respiratory rate and motor activity

In the analyses of respiratory rate, and respiratory and postural motor activities across sleep–wake states, a total of 34,063 epochs were included. These 5 s epochs constitute a total of 47.3 h of data, and 65.7% of all epochs recorded. Of this total, 8374 epochs were from periods of quiet wakefulness, 20,358 were from non-REM sleep and 5331 were from REM sleep. Also of the total number of epochs, 17,472; 11,426; and 5165 were obtained during microperfusion of ACSF, 8-OH-DPAT, and WAY 100135 perfusion into the PPTn, respectively.

Figure 6 shows an example of the effects of microperfusion of 8-OH-DPAT into the PPTn on respiratory rate and motor activities across sleep–wake states. Note the increased respiratory rate and respiratory-related genioglossus activity across all sleep–wake states, and the increased sporadic motor activations occurring during REM sleep in the presence of 8-OH-DPAT compared with ACSF. Group data are shown in Figure 7.

Respiratory rate

There was a significant effect of intervention at the PPTn on respiratory rate (main effect of Treatment: $F_{(1,11)} = 14.00$, $p = 0.003$, two-way ANOVA-RM), with rate increasing in the presence of 8-OH-DPAT compared with the ACSF controls ($p =$

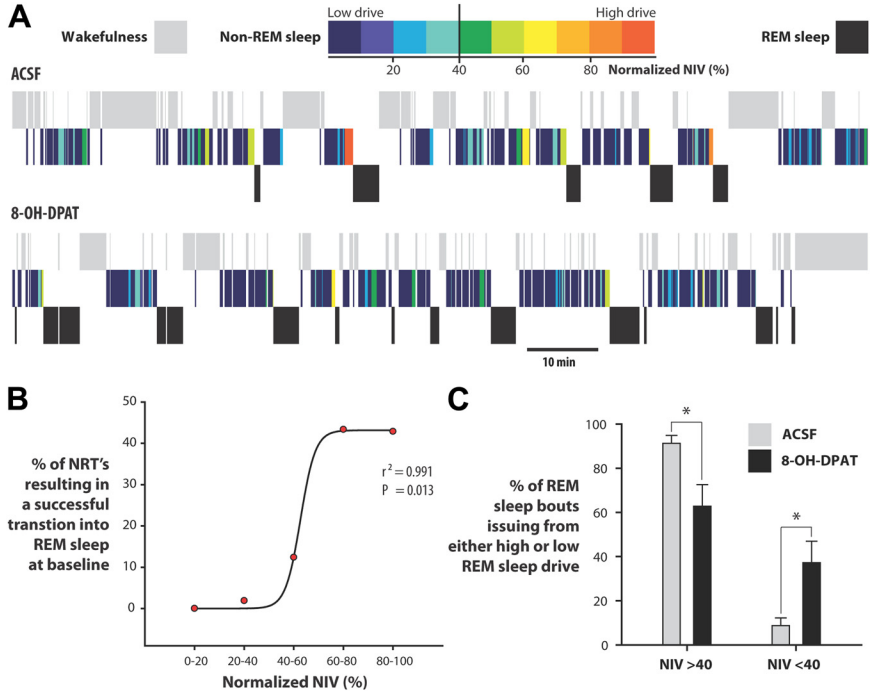

Figure 4. 5-HT$_{1A}$ receptor-responsive PPTn neurons increase the threshold for REM sleep initiation. ***A***, Same hypnograms as from Figure 1*A* but with color coding of the non-REM sleep periods according to the calculated NIV, an index of REM sleep drive. Note that in the presence of 8-OH-DPAT at the PPTn, the REM sleep periods are preceded by NIVs of lower value compared with the ACSF control (i.e., the normal colors before transitions to REM sleep are "blue shifted"). ***B***, The sigmoid relationship between the calculated NIVs and the percentage of NRTs culminating in REM sleep bouts at baseline (i.e., with ACSF at the PPTn); high NIVs are associated with high probabilities of REM sleep onsets. ***C***, The proportion of REM sleep episodes resulting from periods of high REM sleep drive (NIV >40%) significantly decreased with 8-OH-DPAT at the PPTn. Reciprocally, the proportion of REM sleep episodes resulting from periods of low REM sleep drive (NIV <40%) was significantly increased with 8-OH-DPAT at the PPTn. These data show that transitions from non-REM to REM sleep were initiated at lower NIVs in the presence of 8-OH-DPAT at the PPTn, and that 5-HT$_{1A}$ receptor-responsive PPTn neurons therefore normally act to suppress REM sleep by increasing the threshold for its initiation, thereby preventing premature REM sleep transitions. Values are means ± SEM. *$p < 0.05$.

0.003, *post hoc* paired *t* test, Fig. 7*A*). Importantly, this effect of 8-OH-DPAT on respiratory rate was independent of the prevailing sleep–wake state (interaction effect between Treatment and State: $F_{(2,22)} = 0.56$, $p = 0.579$, two-way ANOVA-RM), i.e., occurred in wakefulness, non-REM and REM sleep. There was the expected effect of sleep–wake state per se on respiratory rate (main effect of State: $F_{(2,22)} = 14.75$, $p < 0.001$, two-way ANOVA-RM), with rate increasing in REM sleep compared with both non-REM sleep and wakefulness (both $p < 0.005$, *post hoc* paired *t* tests). WAY 100135 microperfusion into the PPTn did not significantly affect respiratory rate (main effect of Treatment: $F_{(1,10)} = 2.79$, $p = 0.156$, two-way ANOVA-RM).

Respiratory genioglossus activity

Similar to the effects on respiratory rate, there was a significant effect of 8-OH-DPAT intervention at the PPTn on respiratory genioglossus activity (main effect of Treatment: $F_{(1,10)} = 6.69$, $p = 0.027$, two-way ANOVA-RM), with genioglossus activity increasing in the presence of 8-OH-DPAT compared with the ACSF controls ($p = 0.027$, *post hoc* paired *t* test, Fig. 7*B*). Importantly, this effect of 8-OH-DPAT on genioglossus activity was independent of the prevailing sleep–wake state (interaction effect between Treatment and State: $F_{(2,20)} = 0.19$, $p = 0.828$, two-way ANOVA-RM), i.e., occurred in wakefulness, non-REM and REM sleep. There was an effect of sleep–wake state per se on respiratory genioglossus activity (main effect of State: $F_{(2,20)} = 4.69$, $p = 0.021$, two-way ANOVA-RM), with such activity being significantly reduced in REM sleep compared with wakefulness ($p = 0.024$, *post hoc* paired *t* test). There was also a significant effect of WAY 100135 intervention at the PPTn on respiratory genioglossus activity (main effect of Treatment: $F_{(1,10)} = 43.88$, $p = 0.001$, two-way ANOVA-RM) which was sleep-state dependent (interaction effect between Treatment and State: $F_{(2,10)} = 4.59$, $p = 0.039$, two-way ANOVA-RM). In contrast to the activating effects of 8-OH-DPAT, WAY 100135 microperfusion resulted in a 18.5% reduction in respiratory genioglossus activity specifically in wakefulness ($p < 0.001$, *post hoc* paired *t* test).

Diaphragm activity

In contrast to the activating and suppressing effects of 8-OH-DPAT and WAY 100135, respectively at the PPTn on respiratory genioglossus activity, there was no effect on the amplitude of rhythmic diaphragm activation in either group (i.e., 8-OH-DPAT and WAY 100135, respectively, main effect of Treatment: $F_{(1,11)} = 1.39$, $p = 0.264$; and $F_{(1,10)} = 0.23$, $p = 0.651$ two-way ANOVA-RM). As expected, there was also no effect of sleep–wake state per se on the amplitude of rhythmic diaphragm activation (8-OH-DPAT and WAY 100135, respectively, main effect of State: $F_{(2,22)} = 2.66$, $p = 0.093$; $F_{(2,10)} = 2.01$, $p = 0.184$, two-way ANOVA-RM).

Tonic genioglossus activity

There was a significant effect of sleep–wake state on tonic genioglossus activity in both 8-OH-DPAT (Fig. 7*D*) and WAY 100135 groups (main effect of State: $F_{(3,33)} = 94.01$, $p < 0.001$; $F_{(3,15)} = 21.10$, $p < 0.001$, respectively, two-way ANOVA-RM), with motor tone in active wakefulness being increased compared with quiet wakefulness, non-REM sleep and REM sleep (all $p \leq 0.001$, *post hoc* paired *t* tests). However, there was no effect of 8-OH-DPAT or WAY 100135 at the PPTn on tonic genioglossus activity (main effect of Treatment: $F_{(1,11)} = 0.72$, $p = 0.415$; $F_{(1,15)} = 0.50$, $p = 0.511$, respectively, two-way ANOVA-RM), nor was there any effect specific to a given sleep–wake state (8-OH-DPAT and WAY 100135, respectively, interaction effect between Treatment and State: $F_{(3,33)} = 1.42$, $p = 0.254$; $F_{(3,15)} = 5.89$, $p = 0.632$, two-way ANOVA-RM).

Neck muscle activity

Similar to tonic genioglossus muscle activity, there was a significant effect of sleep–wake state on neck muscle activity in both 8-OH-DPAT (Fig. 7*E*) and WAY 100135 groups (main effect of State: $F_{(3,33)} = 72.43$, $p < 0.001$; $F_{(3,15)} = 10.62$, $p < 0.001$, respectively, two-way ANOVA-RM), with activity in sleep being reduced compared with levels in active wakefulness (all *p*-values < 0.035, *post hoc* paired *t* tests). However, there was no effect of 8-OH-DPAT or WAY 100135 at the PPTn on neck muscle activity (main effect of Treatment: $F_{(1,11)} = 4.19$, $p = 0.065$; $F_{(1,15)} = 6.20$, $p = 0.055$, respectively, two-way ANOVA-RM), nor was there any effect specific to a given sleep–wake state (8-OH-DPAT

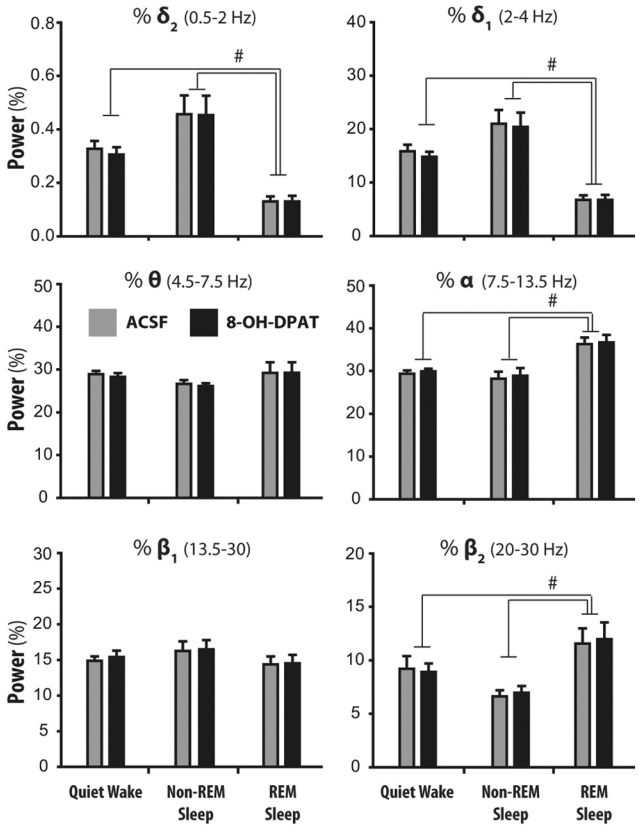

Figure 5. No effect of 8-OH-DPAT at the PPTn on EEG power in any frequency band (0.5–30 Hz) across the states of wakefulness, non-REM and REM sleep. Values are means ± SEM. $^{\#}p < 0.05$ for indicated comparisons between sleep–wake states.

and WAY 100135, respectively, interaction effect between Treatment and State: $F_{(3,33)} = 2.66, p = 0.065$; $F_{(3,15)} = 1.39, p = 0.286$, two-way ANOVA-RM).

Phasic motor events within REM sleep

The amplitude of phasic genioglossus activations in REM sleep was increased with 8-OH-DPAT at the PPTn compared with the ACSF controls ($p = 0.037$, paired t test, Fig. 7*F*). There was no such effect, however, on the amplitude of phasic neck muscle activations ($p = 0.094$, paired t test, Fig. 7*F*). WAY 100135 microperfusion at the PPTn had no effect on REM sleep phasic motor events in the genioglossus muscle ($p = 0.68$, paired t test) or the neck muscle ($p = 0.564$, paired t test).

Discussion

This study tests a mechanism which is at the root of the long-standing model of REM sleep generation and finds the results do not support that model. We used a tool, microperfusion of the 5-HT_{1A} receptor agonist 8-OH-DPAT (10 μM) into the PPTn, which has been shown in cats to selectively silence those PPTn neurons that are specifically activated in REM sleep, while leaving the activity of the wake/REM sleep-active population unaffected (Thakkar et al., 1998). Although 5-HT_{1A} receptor-responsive PPTn neurons are thought to underpin REM sleep generation (see Introduction), a critical test using this tool had not been performed, and based upon the established model a selective inhibition of this REM sleep-active cell population would be expected to suppress REM sleep if they essentially generate the state. The results showed, however, that 5-HT_{1A} receptor-responsive PPTn neurons function to restrain, rather than enhance, REM sleep because their inhibition using this tool increased, rather than decreased, REM sleep.

Local bilateral microperfusion of 8-OH-DPAT into the PPTn caused a robust increase in REM sleep relative to both the within-animal ACSF controls and the time-controls in which ACSF was perfused at the same time of day as the 8-OH-DPAT interventions (Fig. 1). Additional evidence supporting the claim that 5-HT_{1A} receptor-responsive PPTn neurons were mediating the effects on REM sleep comes from the result that the magnitude of the increase in REM sleep produced by the intervention was significantly correlated with the distance of the intervention site from the PPTn (Fig. 2). Our finding of increased REM sleep following an intervention designed to selectively inhibit REM sleep-active PPTn neurons (Thakkar et al., 1998) agrees with other studies which used nonselective approaches to inactivate the PPTn; increased REM sleep occurs after spatially restricted chemical lesions of the PPTn (Lu et al., 2006), and following microinjection of $GABA_A$ receptor agonists into the PPTn (Pal and Mallick, 2004; Torterolo et al., 2006; Pal and Mallick, 2009). Unlike those studies, however, the increased REM sleep reported here is likely not explained as a consequence of an increased total sleep time stemming from an inadvertent inactivation of wakefulness-promoting wake/REM sleep-active PPTn cell population as these are unaffected by 8-OH-DPAT (Thakkar et al., 1998). Even if REM sleep-active PPTn neurons are thought responsible for generating REM sleep as is the prominent explanation, their inhibition with 8-OH-DPAT ought also to reduce REM sleep as a percentage of the total sleep time, independent of any changes in wakefulness, and this simply did not occur (Fig. 1). Moreover, we do not think that the presence of the microdialysis probes at the PPTn per se was responsible for the observed effects on REM sleep in these experiments. Both experimental groups (i.e., 8-OH-DPAT and WAY 100135) had microdialysis probes perfusing the PPT nuclei bilaterally, but importantly so did the time-control group that were perfused bilaterally with ACSF. As shown in Figure 1, there were drug-specific effects occurring in predictable directions, with significant differences between the 8-OH-DPAT, WAY 100135 and ACSF time-control conditions. Such drug-specific effects occurring in predictable directions would not be expected if there were nonspecific effects simply because of the probes (the probe being present in all conditions).

5-HT_{1A} receptor-responsive PPTn neurons and REM sleep drive threshold

The increased REM sleep following bilateral microperfusion of 8-OH-DPAT into the PPTn was the result of an increased frequency of REM sleep bouts and not their duration, so indicating an effect on mechanisms of REM sleep initiation but not maintenance (Benington and Heller, 1994; Benington et al., 1994). This result suggests that during normal non-REM to REM sleep transitions when REM sleep-active PPTn neurons increase their activity (Steriade et al., 1990; Steriade and McCarley, 2005a,b), the activation of these cells normally functions to reduce the probability of REM sleep onsets, such that with their experimental inactivation this restraint is removed leading to an increased number of successful initiations of REM sleep.

The logical consequence of such an effect of 5-HT_{1A} receptor-responsive PPTn neurons on mechanisms of REM sleep initiation but not maintenance is that once sufficient REM sleep drive has accumulated to initiate the REM episode, the continued ac-

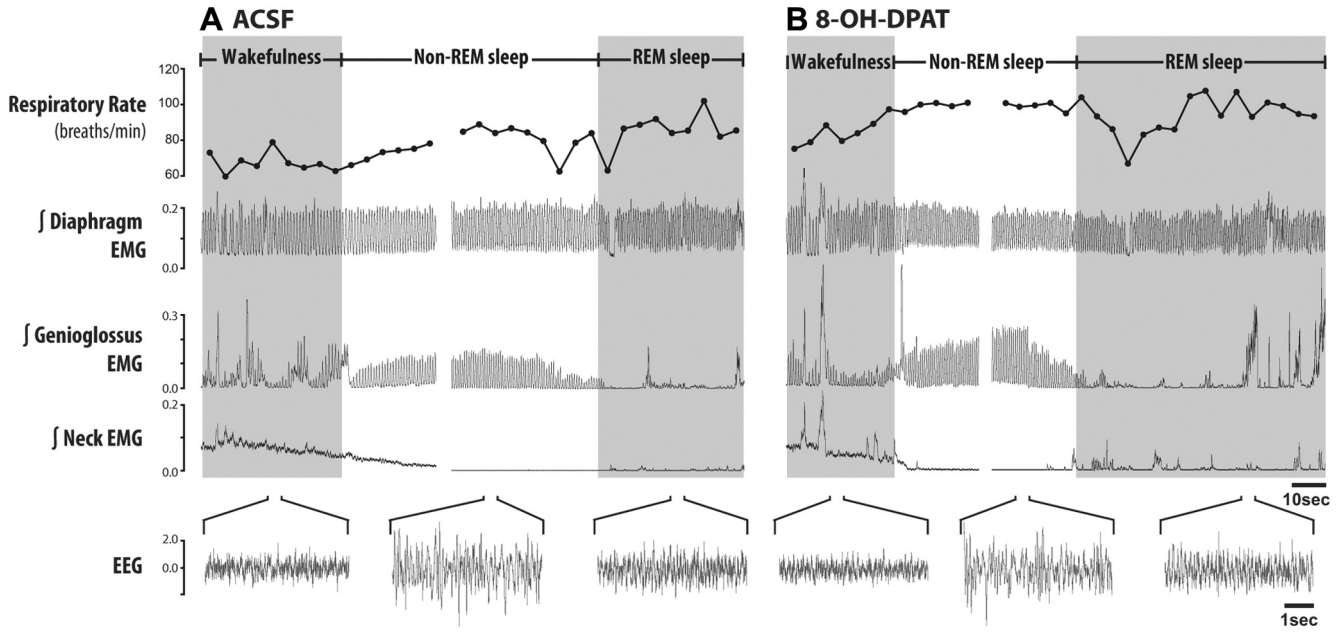

Figure 6. Inhibition of 5-HT_{1A} receptor-responsive PPTn neurons increases respiratory motor activity. ***A***, ***B***, Example traces from a single rat showing the effects of microperfusion of ACSF (***A***) and 8-OH-DPAT (***B***) into the PPTn on respiratory rate and motor activities across sleep–wake states. The tracings are continuous records of activity from wakefulness to non-REM and REM sleep, with the long non-REM period split by a break where indicated. Representative examples of the EEG from each sleep–wake state are shown on a faster time scale where indicated. Note the increased respiratory rate and respiratory-related genioglossus activity with 8-OH-DPAT occurring independently of sleep–wake state, and the increased sporadic motor activations occurring during REM sleep with 8-OH-DPAT compared with ACSF.

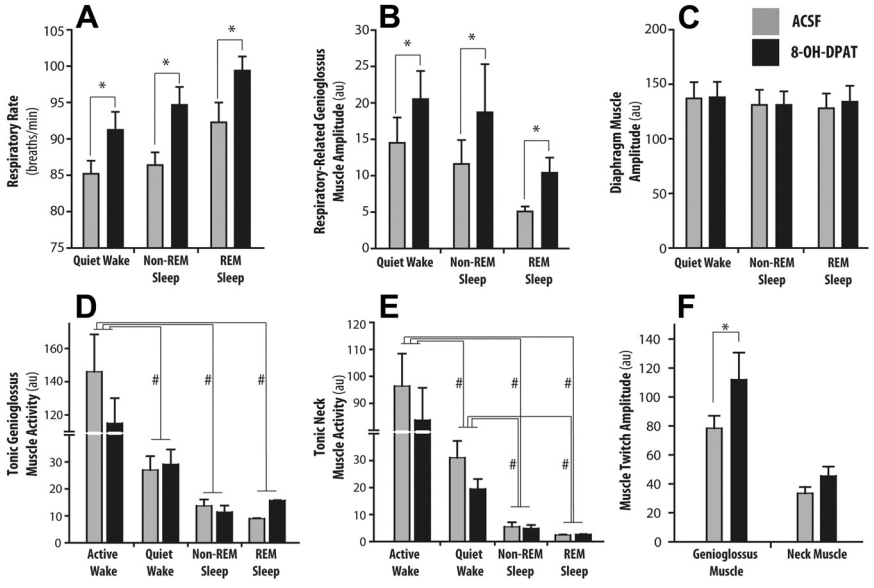

Figure 7. Group data showing the effects of ACSF versus 8-OH-DPAT at the PPTn on respiratory rate and motor activities across sleep–wake states. Note the significant increases in respiratory rate (***A***) and respiratory-related genioglossus activity (***B***) occurring with 8-OH-DPAT at the PPTn independent of the prevailing sleep–wake state, i.e., occurring in wakefulness, non-REM, and REM sleep. In contrast, there was no effect of 8-OH-DPAT at the PPTn on the amplitude of rhythmic diaphragm activation (***C***), or tonic genioglossus (***D***) and neck muscle activities (***E***). The amplitude of phasic genioglossus activations in REM sleep was also increased with 8-OH at the PPTn compared with the ACSF controls, but not so for the amplitude of phasic neck muscle activations (***F***). Values are means ± SEM. *$p < 0.05$ from within-animal baseline ACSF control; $^{\#}p < 0.05$ for indicated comparisons between sleep–wake states.

tivity of such REM sleep-active PPTn neurons is functionally unable to restrain the continued maintenance of that episode. This effect can be most simply explained if a different population of neurons is involved in REM sleep generation, i.e., not the 5-HT_{1A} receptor-responsive PPTn population, the influence of which restrains rather than promotes REM sleep (discussed above).

We used the magnitude of the stereotypical electroencephalographic changes that herald the onset of REM sleep as an indicator of the magnitude of drive for REM sleep. That the NIV is a valid index of REM sleep drive is based on previous work (Benington and Heller, 1994; Benington et al., 1994) and the positive association between the NIV index and successful transitions into REM sleep (Fig. 4). We then showed that during local microperfusion of 8-OH-DPAT into the PPTn there was a significant increase in the proportion of REM sleep bouts stemming from periods of low REM sleep drive (i.e., with low NIV values). This effect is consistent with 5-HT_{1A} receptor-responsive PPTn neurons functioning to normally suppress transitions into REM sleep by elevating the drive threshold for REM sleep induction, such that when this drive threshold is lowered by inhibition of these neurons, REM sleep transitions are initiated at lower drives. In all other respects, the REM sleep episodes (as well as the non-REM sleep and waking episodes) in the presence of 8-OH-DPAT were normal, as judged by no change in EEG frequencies, postural muscle tone (Figs. 5, 7) or behavior as noted from the video recordings.

Overall, these results suggest that 5-HT_{1A} receptor-responsive PPTn neurons function to prevent premature transitions into REM sleep, and so constrain the occurrence of this state to narrow temporal windows of high REM sleep drive, by maintaining a high drive threshold for REM sleep induction. Consistent with

this interpretation is the absence of a REM sleep effect during WAY 100135 microperfusion of the PPTn. 5-HT_{1A} receptor antagonism would be expected to increase activity of REM sleep-active 5-HT_{1A} receptor-responsive PPTn neurons mainly during wakefulness when serotonergic input is high, and have no effect at transitions into and during REM sleep when serotonergic input is low (Lydic et al., 1983; Tsunematsu et al., 2011). Nevertheless, the effective state dependency of 5-HT_{1A} receptor antagonism at the PPTn is evidenced by the inhibition of respiratory genioglossus activity by WAY 100135 microperfusion during wakefulness only, reversing the activation of respiratory measures produced by 8-OH-DPAT. In contrast, increasing REM sleep drive threshold during wakefulness with WAY 100135 could not reduce the occurrence of REM sleep as there is no REM sleep at that time. It is worth noting, however, that if 5-HT_{1A} receptor-responsive PPTn neurons were REM sleep promoting or wake promoting (i.e., wake/REM sleep active) then changes in sleep architecture would be expected during WAY 100135 microperfusion at the PPTn but this did not occur.

Mechanism to explain how 5-HT_{1A} receptor-responsive PPTn neurons suppress REM sleep

Our proposal that the 5-HT_{1A} receptor-responsive (REM sleep-active) PPTn cell population is a negative regulator of REM sleep is inconsistent with the model suggesting that these cells provide cholinergic innervation and activation of the PRF neurons that gate entry into REM sleep (Hobson et al., 2000; Lydic and Baghdoyan, 2003; Steriade and McCarley, 2005b). The original study that provided the precedent for microperfusion of 10 μM 8-OH-DPAT into the PPTn, to selectively silence REM sleep-active PPTn neurons, however, was performed in cats (Thakkar et al., 1998), whereas our study was performed in rats. Nevertheless, if the long-standing model of REM sleep generation is correct in positing that 8-OH-DPAT-sensitive REM sleep-active PPTn neurons promote REM sleep in cats, then our data do not support the primacy and generality of that mechanism when tested in rats. This lack of consistency with that long-standing model, however, does not reflect a lack of agreement between our data and those of others which together can explain REM sleep regulation.

Cholinergic REM sleep-active PPTn neurons account for only a small proportion (4–14%) of the total REM sleep-active PPTn cell population (Maloney et al., 1999; Verret et al., 2005) especially when compared with the proportion of GABAergic REM sleep-active PPTn neurons (44–76%) (Maloney et al., 2002; Sapin et al., 2009). Although 5-HT_{1A} receptor mRNA is present in the PPTn (Wright et al., 1995) it was not detected in rodent cholinergic PPTn neurons but was expressed by PPTn GABAergic neurons (Bonnavion et al., 2010). Although a previous study has shown that 5-HT inhibits cholinergic PPTn neurons *in vitro* (Leonard and Llinás, 1994), (±)8-OH-DPAT produced no effect in four of four cholinergic neurons tested whereas two neurons were hyperpolarized by (+)8-OH-DPAT. It is not known whether those cholinergic neurons studied *in vitro* constitute the REM sleep-active PPTn population inhibited by (±)8-OH-DPAT *in vivo* (Thakkar et al., 1998).

The observed increase in REM sleep following selective suppression of 5-HT_{1A} receptor-responsive (REM sleep-active) PPTn neurons is consistent with the model that withdrawal of GABA release at downstream sites is critically involved in REM sleep generation. Blocking the action of endogenous GABA at the sublaterodorsal nucleus induces REM sleep, while local application of $GABA_A$ receptor agonists suppresses REM sleep (Boissard et al., 2002; Pollock and Mistlberger, 2003; Sanford et al., 2003; Sapin et al., 2009). Given that the PPTn is a source of GABAergic innervation of the sublaterodorsal nucleus (Boissard et al., 2003; Lu et al., 2006), REM sleep-active PPTn neurons can suppress REM sleep initiation by suppressing the excitability of REM sleep-active sublaterodorsal nucleus neurons via increased GABA release during non-REM to REM sleep transitions.

5-HT_{1A} receptor-responsive PPTn neurons suppress respiratory activity

REM sleep-active PPTn neurons also shape the expression of the phenomenological components of REM sleep, with the focus of the present study being respiratory network activity given the relevance of sleep-disordered breathing in REM sleep. We showed a robust increase in both respiratory rate and respiratory-related genioglossus muscle activity, and increases in the frequency and amplitude of sporadic genioglossus activations in REM sleep following targeted inhibition of 5-HT_{1A} receptor-responsive PPTn neurons with 8-OH-DPAT (Thakkar et al., 1998). In contrast, microperfusion of the 5-HT_{1A} receptor antagonist into the PPTn decreased respiratory genioglossus activity. These data therefore indicate that 5-HT_{1A} receptor-responsive PPTn neurons also function to normally restrain respiratory rate and motor activities, with release of this restraint leading to augmentations of these components of respiratory activity. It remains to be determined whether this restraining effect is also due to alterations in GABA release at sites in the respiratory network due to the manipulations at the PPTn, as discussed above in explaining the effects on REM sleep.

Of note, the increases in respiratory rate and genioglossus muscle activity with 8-OH-DPAT at the PPTn occurred not only during REM sleep, but also during non-REM sleep and wakefulness (Fig. 7). This is explained because although discharging maximally during REM sleep, 5-HT_{1A} receptor-responsive PPTn neurons are also moderately active during wakefulness and non-REM sleep with this activation suppressed by 8-OH-DPAT (Steriade et al., 1990; Thakkar et al., 1998). The PPTn possesses the necessary connectivity to the respiratory network, with projections to the hypoglossal motor pool and premotor sites (Woolf and Butcher, 1989; Fay and Norgren, 1997), and the rostral-ventrolateral medulla (Yasui et al., 1990) which houses the circuitry for respiratory rhythm generation (Feldman and Del Negro, 2006).

References

Amici R, Domeniconi R, Jones CA, Morales-Cobas G, Perez E, Tavernese L, Torterolo P, Zamboni G, Parmeggiani PL (2000) Changes in REM sleep occurrence due to rhythmical auditory stimulation in the rat. Brain Res 868:241–250.

Benington JH, Heller HC (1994) REM-sleep timing is controlled homeostatically by accumulation of REM-sleep propensity in non-REM sleep. Am J Physiol 266:R1992–R2000.

Benington JH, Kodali SK, Heller HC (1994) Scoring transitions to REM sleep in rats based on the EEG phenomena of pre-REM sleep: an improved analysis of sleep structure. Sleep 17:28–36.

Bevan MD, Bolam JP (1995) Cholinergic, GABAergic, and glutamate-enriched inputs from the mesopontine tegmentum to the subthalamic nucleus in the rat. J Neurosci 15:7105–7120.

Boissard R, Gervasoni D, Schmidt MH, Barbagli B, Fort P, Luppi PH (2002) The rat ponto-medullary network responsible for paradoxical sleep onset and maintenance: a combined microinjection and functional neuroanatomical study. Eur J Neurosci 16:1959–1973.

Boissard R, Fort P, Gervasoni D, Barbagli B, Luppi PH (2003) Localization of the GABAergic and non-GABAergic neurons projecting to the sublaterodorsal nucleus and potentially gating paradoxical sleep onset. Eur J Neurosci 18:1627–1639.

Bonnavion P, Bernard JF, Hamon M, Adrien J, Fabre V (2010) Heteroge-

neous distribution of the serotonin 5-HT(1A) receptor mRNA in chemically identified neurons of the mouse rostral brainstem: implications for the role of serotonin in the regulation of wakefulness and REM sleep. J Comp Neurol 518:2744–2770.

Bourgin P, Escourrou P, Gaultier C, Adrien J (1995) Induction of rapid eye movement sleep by carbachol infusion into the pontine reticular formation in the rat. Neuroreport 6:532–536.

Chan E, Steenland HW, Liu H, Horner RL (2006) Endogenous excitatory drive modulating respiratory muscle activity across sleep-wake states. Am J Respir Crit Care Med 174:1264–1273.

Deurveilher S, Hars B, Hennevin E (1997) Pontine microinjection of carbachol does not reliably enhance paradoxical sleep in rats. Sleep 20:593–607.

Fay RA, Norgren R (1997) Identification of rat brainstem multisynaptic connections to the oral motor nuclei using pseudorabies virus. III. Lingual muscle motor systems. Brain Res Brain Res Rev 25:291–311.

Feldman JL, Del Negro CA (2006) Looking for inspiration: new perspectives on respiratory rhythm. Nat Rev Neurosci 7:232–242.

Fletcher A, Cliffe IA, Dourish CT (1993) Silent 5-HT1A receptor antagonists: utility as research tools and therapeutic agents. Trends Pharmacol Sci 14:41–48.

Hobson JA, Pace-Schott EF, Stickgold R (2000) Dreaming and the brain: toward a cognitive neuroscience of conscious states. Behav Brain Sci 23:793–842.

Horner RL, Sanford LD, Annis D, Pack AI, Morrison AR (1997) Serotonin at the laterodorsal tegmental nucleus suppresses rapid-eye-movement sleep in freely behaving rats. J Neurosci 17:7541–7552.

Horner RL, Brooks D, Kozar LF, Leung E, Hamrahi H, Render-Teixeira CL, Makino H, Kimoff RJ, Phillipson EA (1998) Sleep architecture in a canine model of obstructive sleep apnea. Sleep 21:847–858.

Jones BE (1990) Immunohistochemical study of choline acetyltransferase-immunoreactive processes and cells innervating the pontomedullary reticular formation in the rat. J Comp Neurol 295:485–514.

Kohlmeier KA, Burns J, Reiner PB, Semba K (2002) Substance P in the descending cholinergic projection to REM sleep-induction regions of the rat pontine reticular formation: anatomical and electrophysiological analyses. Eur J Neurosci 15:176–196.

Leonard CS, Llinás R (1994) Serotonergic and cholinergic inhibition of mesopontine cholinergic neurons controlling REM sleep: an in vitro electrophysiological study. Neuroscience 59:309–330.

Lu J, Sherman D, Devor M, Saper CB (2006) A putative flip-flop switch for control of REM sleep. Nature 441:589–594.

Lydic R, Baghdoyan HA (2003) Neurochemical evidence for the cholinergic modulation of sleep and breathing. In: Sleep-related breathing disorders: experimental models and therapeutic potential (Carley DW, Radulovacki M, eds), pp 57–91. New York: Dekker.

Lydic R, McCarley RW, Hobson JA (1983) The time-course of dorsal raphe discharge, PGO waves, and muscle tone averaged across multiple sleep cycles. Brain Res 274:365–370.

Maloney KJ, Mainville L, Jones BE (1999) Differential c-Fos expression in cholinergic, monoaminergic, and GABAergic cell groups of the pontomesencephalic tegmentum after paradoxical sleep deprivation and recovery. J Neurosci 19:3057–3072.

Maloney KJ, Mainville L, Jones BE (2002) c-Fos expression in dopaminergic and GABAergic neurons of the ventral mesencephalic tegmentum after paradoxical sleep deprivation and recovery. Eur J Neurosci 15:774–778.

Morrison JL, Sood S, Liu X, Liu H, Park E, Nolan P, Horner RL (2002) Glycine at hypoglossal motor nucleus: genioglossus activity, CO(2) responses, and the additive effects of GABA. J Appl Physiol 93:1786–1796.

Pal D, Mallick BN (2004) GABA in pedunculopontine tegmentum regulates spontaneous rapid eye movement sleep by acting on GABAA receptors in freely moving rats. Neurosci Lett 365:200–204.

Pal D, Mallick BN (2009) GABA in pedunculopontine tegmentum increases rapid eye movement sleep in freely moving rats: possible role of GABAergic inputs from substantia nigra pars reticulata. Neuroscience 164:404–414.

Paxinos G, Watson C (1998) The rat brain in stereotaxic coordinates, Ed 4. San Diego: Academic.

Pollock MS, Mistlberger RE (2003) Rapid eye movement sleep induction by microinjection of the GABA-A antagonist bicuculline into the dorsal subcoeruleus area of the rat. Brain Res 962:68–77.

Pollock MS, Mistlberger RE (2005) Microinjection of neostigmine into the pontine reticular formation of the mouse: further evaluation of a proposed REM sleep enhancement technique. Brain Res 1031:253–267.

Rukhadze I, Kubin L (2007) Mesopontine cholinergic projections to the hypoglossal motor nucleus. Neurosci Lett 413:121–125.

Rye DB, Saper CB, Lee HJ, Wainer BH (1987) Pedunculopontine tegmental nucleus of the rat: cytoarchitecture, cytochemistry, and some extrapyramidal connections of the mesopontine tegmentum. J Comp Neurol 259:483–528.

Sanford LD, Tang X, Xiao J, Ross RJ, Morrison AR (2003) GABAergic regulation of REM sleep in reticularis pontis oralis and caudalis in rats. J Neurophysiol 90:938–945.

Sapin E, Lapray D, Bérod A, Goutagny R, Léger L, Ravassard P, Clément O, Hanriot L, Fort P, Luppi PH (2009) Localization of the brainstem GABAergic neurons controlling paradoxical (REM) sleep. PLoS One 4:e4272.

Semba K, Fibiger HC (1992) Afferent connections of the laterodorsal and the pedunculopontine tegmental nuclei in the rat: a retro- and anterograde transport and immunohistochemical study. J Comp Neurol 323:387–410.

Semba K, Reiner PB, Fibiger HC (1990) Single cholinergic mesopontine tegmental neurons project to both the pontine reticular formation and the thalamus in the rat. Neuroscience 38:643–654.

Sood S, Morrison JL, Liu H, Horner RL (2005) Role of endogenous serotonin in modulating genioglossus muscle activity in awake and sleeping rats. Am J Respir Crit Care Med 172:1338–1347.

Steenland HW, Liu H, Horner RL (2008) Endogenous glutamatergic control of rhythmically active mammalian respiratory motoneurons *in vivo*. J Neurosci 28:6826–6835.

Steriade M, McCarley RW (2005a) Neuronal activities in brainstem and basal forebrain structures controlling waking and sleep states. In: Brainstem control of wakefulness and sleep, Ed 2, pp 381–416. New York: Plenum.

Steriade M, McCarley RW (2005b) Neuronal control of REM sleep. In: Brainstem control of wakefulness and sleep, Ed 2, pp 461–511. New York: Plenum.

Steriade M, Datta S, Paré D, Oakson G, Curró Dossi RC (1990) Neuronal activities in brain-stem cholinergic nuclei related to tonic activation processes in thalamocortical systems. J Neurosci 10:2541–2559.

Thakkar MM, Strecker RE, McCarley RW (1998) Behavioral state control through differential serotonergic inhibition in the mesopontine cholinergic nuclei: a simultaneous unit recording and microdialysis study. J Neurosci 18:5490–5497.

Torterolo P, Morales FR, Chase MH (2002) GABAergic mechanisms in the pedunculopontine tegmental nucleus of the cat promote active (REM) sleep. Brain Res 944:1–9.

Torterolo P, Sampogna S, Morales FR, Chase MH (2006) MCH-containing neurons in the hypothalamus of the cat: searching for a role in the control of sleep and wakefulness. Brain Res 1119:101–114.

Tsunematsu T, Kilduff TS, Boyden ES, Takahashi S, Tominaga M, Yamanaka A (2011) Acute optogenetic silencing of orexin/hypocretin neurons induces slow-wave sleep in mice. J Neurosci 31:10529–10539.

Verret L, Léger L, Fort P, Luppi PH (2005) Cholinergic and noncholinergic brainstem neurons expressing Fos after paradoxical (REM) sleep deprivation and recovery. Eur J Neurosci 21:2488–2504.

Vincent SR, Satoh K, Armstrong DM, Fibiger HC (1983) NADPH-diaphorase: a selective histochemical marker for the cholinergic neurons of the pontine reticular formation. Neurosci Lett 43:31–36.

Woolf NJ, Butcher LL (1989) Cholinergic systems in the rat brain: IV. Descending projections of the pontomesencephalic tegmentum. Brain Res Bull 23:519–540.

Wright DE, Seroogy KB, Lundgren KH, Davis BM, Jennes L (1995) Comparative localization of serotonin1A, 1C, and 2 receptor subtype mRNAs in rat brain. J Comp Neurol 351:357–373.

Yasui Y, Cechetto DF, Saper CB (1990) Evidence for a cholinergic projection from the pedunculopontine tegmental nucleus to the rostral ventrolateral medulla in the rat. Brain Res 517:19–24.

Younes M, Park E, Horner RL (2007) Pentobarbital sedation increases genioglossus respiratory activity in sleeping rats. Sleep 30:478–488.